ELSEVIER

Journal of Molecular Catalysis A: Chemical 162 (2000) 353–365

JOURNAL OF MOLECULAR CATALYSIS A: CHEMICAL

www.elsevier.com/locate/molcata

Sol–gel synthesis, characterization by solid state NMR and HDS activity of Mo–alumina and Mo–P–alumina based catalysts

Juliette Quartararo [a], Jean-Paul Amoureux [b], Jean Grimblot [a,*]

[a] *Laboratoire de catalyse, UPRESA 8010, Université des Sciences et Technologies de Lille, Bâtiment C_3, 59655 Villeneuve d'Ascq Cédex, France*

[b] *Laboratoire de dynamique et structure des matériaux moléculaires, UPRESA 8024, Université des Sciences et Technologies de Lille, Bâtiment P_5, 59655 Villeneuve d'Ascq Cédex, France*

Special issue dedicated to Professor H. Knözinger.

Abstract

The aim of the present study was to prepare different Mo–alumina and Mo–P–alumina catalysts by a sol–gel method. The wishes were to underline the influence of the way to introduce the different Mo and/or P elements in the architecture of the dried and calcined solids and the consequences on their catalytic properties. During the sol–gel alumina synthesis, molybdenum [precursor = $(NH_4)_6Mo_7O_{24} \cdot 4H_2O$] and phosphorus (precursor = H_3PO_4) can be introduced separately or simultaneously in 2-butanol (step 1) or in water (step 3) to obtain the final mixed oxide. For Mo–alumina, the influence of the amount of molybdenum (Mo/Al ratio = 0.1, 0.2 or 0.3) has been studied, whereas for the Mo–P–Al solids, four combinations have been prepared with a fixed Mo/Al ratio at 0.2 and P/Al ratio at 0.03 and 0.2. The dried and calcined samples have been extensively characterized by ^{27}Al, ^{31}P MAS NMR and ^{27}Al Multiple Quantum Magic Angle Spinning NMR (MQMAS NMR). After sulfidation, the solids have been tested in hydrodesulfurization (HDS) of thiophene.

It appears that the activity of Mo–Al catalysts increases when the molybdenum amount increases and when molybdenum is dissolved in 2-butanol during the synthesis.

A promotor effect of phosphorus has been observed in some cases, particularly, when the molybdenum and the phosphorus precursors are both dissolved in water. Moreover, this study has shown the importance of the step of introduction of phosphorus for the catalytic performances of the Mo–P–Al catalysts. These catalytic results are correlated with some nuclear magnetic resonance (NMR) characterizations, which evidence the formation of different aluminium phosphates.

Keywords: Sol–gel synthesis; NMR and HDS activity; Mo–alumina and Mo–P–alumina based catalysts

* Corresponding author. Tel.: +33-3-20-43-45-38; fax: +33-3-20-43-65-61.
E-mail address: jean.grimblot@univ-lille1.fr (J. Grimblot).

1381-1169/00/$ - see front matter
PII: S1381-1169(00)00302-2

1. Introduction

Hydrotreating catalysts (HDT) are devoted to remove the heteroatoms, like sulfur (hydrodesulfurization; HDS), nitrogen (hydrodenitrogenation; HDN) or some metals (Ni, V; hydrodemetallation; HDM) present in the petroleum fractions with the aim to produce low polluting fuels. Classically, after activation, the catalysts are constituted by an active MoS_2 phase promoted by Co or Ni and supported by γ-alumina [1,2].

Usually, the oxide precursor of HDT catalysts are prepared by simultaneous or consecutive dry impregnation of an alumina support, with aqueous solutions containing the element Mo, Co or Ni as ammonium molybdate, cobalt or nickel nitrate. The impregnated alumina is then calcined to produce the oxidic form of the catalysts. An alternative choice of the preparation of these oxides is the sol–gel method using an aluminium alcoxide precursor [3,4]. This method permits to increase the molybdenum amount and leads to solids with high specific surface area (SSA).

Moreover, a recent study of mixed P–Al oxides [5] has shown that the sol–gel method permits to control the formation of different phosphates species. However, the role of phosphorus in HDT catalysts, such as Mo/Al_2O_3 or $Co(Ni)–Mo/Al_2O_3$ is still subject of studies and controversial discussions [6–14].

The main aim of this work is to study the influence of the presence of phosphorus during the sol–gel synthesis of Mo–alumina catalysts. Two aspects will be considered: (i) the catalytic performances using HDS of thiophene as a model test, and (ii) the identifications of the local structural environments of the introduced elements and the corresponding phases by X-ray diffraction (XRD) and solid state nuclear magnetic resonance (NMR). Indeed, due to the rather amorphous character of such solids, NMR has been proven to be an interesting tool [5,15,16]. In particular, to identify local Al sites, two-dimensional (2D) ^{27}Al Multiple Quantum Magic Angle Spinning NMR (2D-MQMAS NMR) has been used. The main parameter, which has revealed some influence on these two last aspects, is the step at which the elements P and/or Mo are introduced during the procedure of sol–gel synthesis. Despite the fact that the active catalysts are in a sulfided form such as (P) MoS_2-alumina, the NMR characterizations were mainly performed on the oxide solids.

2. Experimental

2.1. Catalysts preparation

The preparation of the catalysts has been conducted according to a sol–gel procedure already described [3,4,7] to obtain pure alumina and alumina modified by Mo or by Mo and P. The alumina framework was obtained by hydrolysis of aluminium-tri *sec* butylate [ASB, $Al(OC_4H_9)_3$] (from Fluka, purity ≥ 95%) dissolved first in its parent alcohol (2-butanol, from Fluka, purity ≥ 99.5%). 1,3-Butanediol (from Fluka, purity ≥ 98%), which is acting as a chelating agent, was then added to the initial solution to better control the hydrolysis step, which was conducted with distilled water. After stirring the mixture for 1 h at 85°C and holding the gel with the solution at room temperature for 1 h, the solids were dried in two steps at 40°C and then at 100°C in open air. At this stage, the solids will be labelled with "D". The next step is calcination in flowing air in a quartz reactor at typically 500°C for 3 h, unless otherwise stated. The final oxides will be labelled with "C".

For the preparation of P–alumina supports [5], the phosphorus precursor (H_3PO_4) was introduced in step 1 (solids X1-Al), in step 2 (solids X2-Al) or in step 3 (solids X3-Al) as reported in Fig. 1. Here, we will restrict the study to the introduction of the precursors of P and/or Mo in steps 1 and/or 3.

For the Mo–Al solids, the molybdenum precursor [$(NH_4)_6Mo_7O_{24} \cdot 4H_2O$ from Fluka] was introduced at two different stages of the sample synthesis. In the sample nomenclature, Mo1 or Mo3 designates the step of dissolution (1 in 2-butanol; 3 in water) and the value in parenthesis indicates the atomic ratio Mo/Al, namely Mo/Al = 0.1, 0.2 and 0.3.

For the Mo–P–Al solids, the phosphorus precursor (H_3PO_4 from Fluka, a solution containing 85% of phosphoric acid) is also introduced at two different steps of the synthesis, in 2-butanol (step 1) or in water (step 3). For example, for a solid named Mo1P3–Al, molybdenum is introduced in step 1

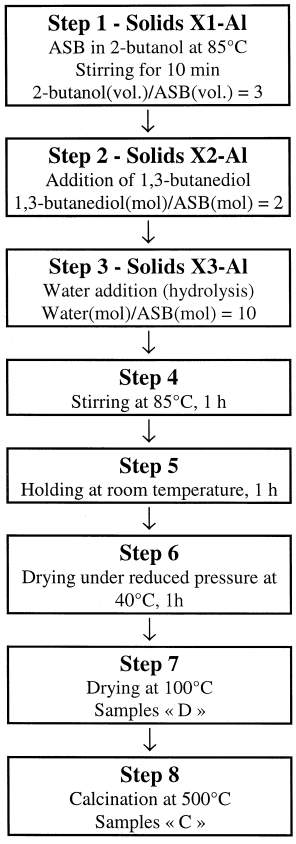

Fig. 1. Schematic description of the procedure to prepare Mo–P–alumina mixed oxides (from Ref. [5]). In the present study, the Mo or P precursors are introduced in step 1 (samples X1-Al) or in step 3 (samples X3-Al).

(2-butanol) and phosphorus in step 3 (water). For these mixed oxides, the molybdenum amount is maintained constant and corresponds to a Mo/Al atomic ratio = 0.2 and the P/Al atomic ratio are, respectively, 0.03 and 0.2.

2.2. Solids characterization

The chemical composition of the calcined mixed oxides was provided by the "Service Central d'Analyses du CNRS" (Vernaison, France).

SSAs were determined by the BET method.

XRD patterns were obtained with a Siemens D5000 diffractometer equipped with a goniometer, a monochromator and a Cu X-ray tube.

Conventional MAS NMR spectra of ^{27}Al were obtained with a Bruker ASX400 spectrometer. The resonance frequency was $\nu o = 104.26$ MHz, with a recycling time of 3 s and a short pulse time of 1 μs (flip angle $\approx \pi/12$). The spinning frequency was 15 kHz and $Al(H_2O)_6^{3+}$ was taken as a reference. ^{31}P MAS NMR spectra were obtained from a Bruker ASX100 spectrometer operating at a resonance frequency of $\nu o = 40.53$ MHz with a recycling time of 40 s and a pulse time of 2 μs (flip angle $\approx \pi/6$). The spinning frequency was 12.5 kHz and H_3PO_4 was taken as a reference.

The theoretical aspects of MQMAS NMR can be found in Refs. [17–20]. The MQMAS measurements were performed with a three-pulse z-filter sequence [21]. The spectra were recorded at $\nu o = 104.26$ MHz on the Bruker ASX400 spectrometer. The spinning frequency was 15 kHz. The three pulses have been experimentally optimised: the first hard pulse to 2.1 μs, the second hard pulse to 0.75 μs and the third selective $\approx \pi/2$ pulse to 6 μs.

2.3. Catalytic tests

HDS of thiophene was performed at atmospheric pressure in a flow type reactor packed with 0.4 g of catalyst. The catalysts were presulfided at 400°C for 2 h (temperature increase rate: 360°C/h) with an H_2/H_2S (90/10) gas mixture at a flow rate of 50 ml min^{-1}. Thiophene, purified by vacuum distillation, was introduced in the reactor at constant pressure (50 Torr) with a flow of dried hydrogen (10 ml/min) at atmospheric pressure and the temperature was kept at 400°C. The reaction products (butane and butene) were analysed by gas chromatography. The results are expressed in conversion of thiophene.

3. Results

3.1. Characterization of the samples in the oxide state

3.1.1. Mo–Al samples: dried state

The two series of samples Mo1–Al and Mo3–Al in the dried state show broad diffraction peaks whatever the series and the Mo/Al atomic ratio (0.1–0.3).

They are characteristic of the presence of poorly crystallised boehmite. Such an observation was already proposed for the dried P1–Al, P2–Al and P3–Al samples [5].

The sample compositions are reported in Table 1. The carbon amount of the dried Mo–Al solids varies between 4.6 and 8.2 wt.% whatever the Mo introduction step (Mo1 or Mo3) and its amount.

The ^{27}Al spectra of the series of dried samples are reported in Fig. 2. For Mo/Al = 0.1, 0.2 and 0.3, there is no difference between Mo1–Al and Mo3–Al with a single ^{27}Al signal around ≈ 6 ppm (Fig. 2). This value corresponds to the presence of octahedral aluminium sites [22] in an oxygen environment.

3.1.2. Mo–Al samples: calcined state

As for the dried samples, three Mo compositions are considered. Now, the carbon amount (Table 1) is very low (less than 0.3 wt.%), whatever the procedure to introduce molybdenum and whatever its amount. Similar results were already found for the P–alumina compounds [5]. This means that the calcination procedure is efficient enough to completely destroy the alcoholic fragments remaining in the dried gels.

Whatever the molybdenum content, the XRD patterns indicate the presence of very badly crystallised γ-alumina with a large amorphous character.

From Table 1, it can also be observed that the SSAs of the calcined Mo–Al samples are always lower when Mo is introduced in step 3 instead of step 1 (Fig. 1). On the other hand, the maximum SSA was obtained for the Mo/Al ratio equal to 0.2.

Table 1
Chemical composition of Mo–alumina samples in the dried and calcined states and SSA

Catalysts	wt.% C		wt.% Mo		Mo/Al	SSA (m^2/g)
	D	C	D	C	D and C	C
Mo1(0.1)–Al	5.3	0.1	8.9	11.1	0.1	392
Mo3(0.1)–Al	7.5	0.05	7.6	8.6	0.1	342
Mo1(0.2)–Al	4.8	0.2	14.0	21.0	0.2	555
Mo3(0.2)–Al	6.8	0.3	13.5	20.1	0.2	523
Mo1(0.3)–Al	4.6	0.03	23.6	30.1	0.3	486
Mo3(0.3)–Al	8.2	0.1	22.8	29.7	0.3	351

D = dried state, C = calcined state; SSA determined after calcination at 500°C.

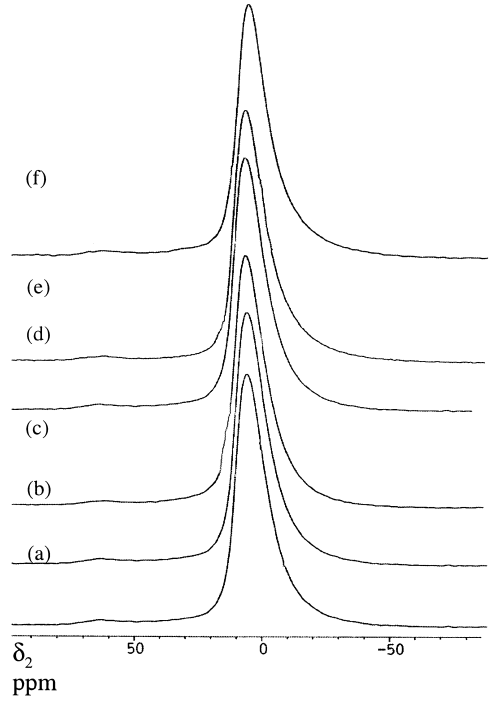

Fig. 2. ^{27}Al MAS NMR spectra of the Mo–Al solids in the dried state: (a) Mo1(0.1)D–Al, (b) Mo3(0.1)D–Al, (c) Mo1(0.2)D–Al, (d) Mo3(0.2)D–Al, (e) Mo1(0.3)D–Al, (f) Mo3(0.3)D–Al.

Nevertheless, in all the cases, SSA values are higher than 350 m^2/g.

^{27}Al spectra of all the prepared samples are reported in Fig. 3. For the samples with Mo/Al = 0.1, there is no clear difference in ^{27}Al spectra between Mo1 and Mo3 with three peak maxima around $\delta_2^G \approx$ 6, 30 and 64 ppm, corresponding to octahedral, pentacoordinate and tetrahedral aluminium sites in an oxygen environment, respectively [22,23]. Moreover, the ^{27}Al NMR spectrum of the Mo3(0.3)C–Al sample shows the presence of $Al_2(Mo_4)_3 \cdot (\delta_2^G \approx -12.9$ ppm), a phase usually observed for high amounts of molybdenum and high temperatures of calcination [24,25].

3QMAS NMR was performed to better identify the different aluminium sites with their actual isotropic chemical shifts and their quadrupolar interactions in the Mo(0.2)C–Al and Mo(0.3)C–Al sample series. Indeed, when the nucleus spin number is greater than 1/2, the nucleus possesses an electric quadrupole momentum that interacts with the electric field gradients at the nucleus. The resulting

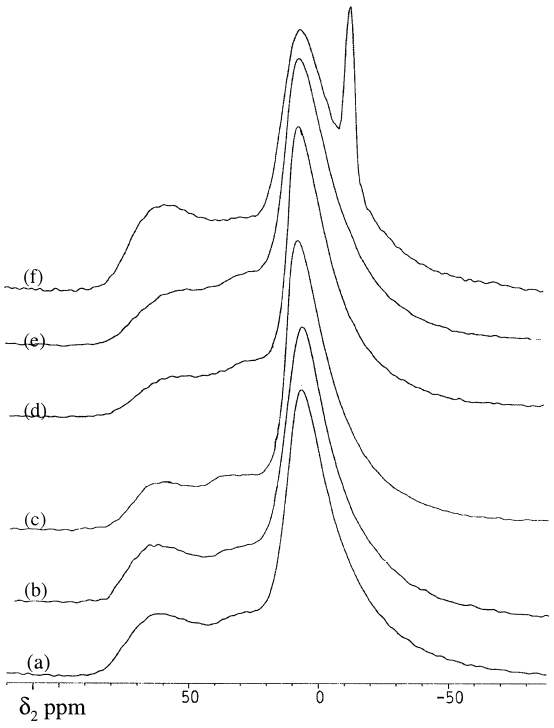

Fig. 3. ^{27}Al MAS NMR spectra of the calcined Mo–Al solids. (a) Mo1(0.1)C–Al, (b) Mo3(0.1)C–Al, (c) Mo1(0.2)C–Al, (d) Mo3(0.2)C–Al, (e) Mo1(0.3)C–Al, (f) Mo3(0.3)C–Al.

quadrupolar effects are strongly linked to the local surrounding symmetry of the nucleus. Apart of the line broadening resulting from the quadrupolar interaction, another important effect can be noted: the resonances are shifted from the true isotropic chemical shifts (δ_{CS}) by the quadrupolar induced shifts (δ_{QIS}), which are dependent on the amplitude of the quadrupole interactions. It follows that corrections must be performed to obtain the actual chemical shifts before carrying out relevant comparison between the various samples. This is possible using MQMAS spectra.

After shearing the 2D 3QMAS spectrum, we can define in parts per million the two principal axes: δ_2 and δ_{iso}. The projection of the 2D spectrum onto the δ_2 axis leads to the one-dimensional (1D) MAS spectrum filtered in 3 Quanta. An orthogonal projection of the 2D spectrum on the δ_{iso} axis leads to the high resolution 1D spectrum.

On the 2D spectra (Fig. 4), we can draw two particular lines: the chemical shift (CS) axis, which gives the location of the resonance (true isotropic chemical shift) in the absence of quadrupolar interaction and the quadrupolar induced shift (QIS) direction [21]. On the one hand, projections of the gravity center of each resonance on the CS axis along the QIS direction (slope $= -10/17$) permit the determination of the actual isotropic chemical shifts (δ_{CS}). On the other hand, the distance of the gravity center from the CS axis along the QIS direction allows to determine the Second Order Quadrupolar Effect (SOQE), SOQE $= C_q\sqrt{1+\eta_Q^2/3}$ [21]. For each species, the actual chemical shift can also be

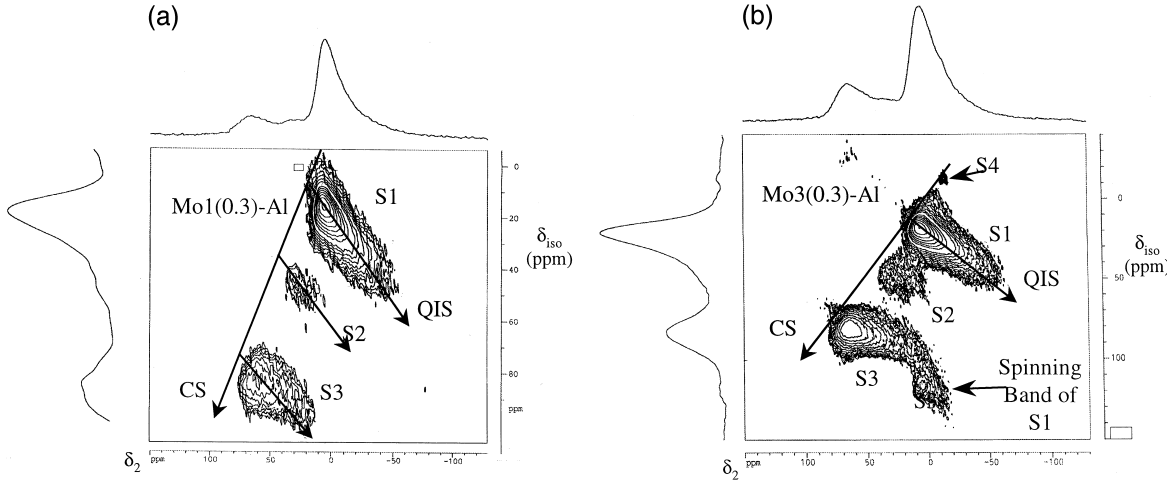

Fig. 4. ^{27}Al 3QMAS NMR sheared spectra of the calcined solids. (a) Mo1(0.3)C–Al, (b) Mo3(0.3)C–Al catalysts.

deduced from the position of the gravity centers (δ_2^G) of its resonance by the relation (for $S = 5/2$):

$$\delta_{CS} = \delta_2^G + \delta_{QIS} = \delta_2^G - 6000(SOQE/\nu o)^2$$

In addition, it can be noticed that if the surrounding of a nucleus is perfectly determined, the corresponding sheared resonance is very narrow and parallel to the δ_2 axis. Conversely, any vertical spreading of the sheared resonances may indicate a distribution of chemical shift and/or quadrupolar interaction.

Fig. 4 reports the typical ^{27}Al 3QMAS NMR spectra of the Mo1(0.3)C–Al and Mo3(0.3)C–Al samples. The corresponding Mo1(0.1), Mo1(0.2) and Mo3(0.2) 2D spectra are similar to the Mo1(0.3)–Al one. Octahedral ($\delta_2^G = 6$ ppm), pentacoordinate ($\delta_2^G = 29$ ppm) and tetrahedral ($\delta_2^G = 64$ ppm) aluminium sites are clearly identified. In case of the Mo3(0.3)C sample, we can observe a fourth species corresponding to the $Al_2(MoO_4)_3$ ($\delta_2^G = -12.9$ ppm), identified in the ^{27}Al MAS spectrum for the higher amount of molybdenum. The intensity of this last specie is weak in the 2D spectra.

The corresponding isotropic chemical shifts and the SOQEs are reported in Table 2. A significant distribution of the octahedral site resonances is also observed preferentially along the QIS direction, which denotes a spreading of the SOQE parameter. Whatever the molybdenum amount, the SOQE values are quite similar for the octahedral aluminium sites (≈ 3.4 MHz). The same trend can be observed for the second species attributed to pentacoordinate aluminium sites (≈ 4.3 MHz). Concerning the tetrahedral species, the SOQE values are around 4.2–4.5 MHz. In case of the Al species in $Al_2(MoO_4)_3$, the SOQE is very low (0.5 MHz) showing the presence of a well symmetrical surrounding for this species. The intensity of the signal of this species is very low in the 3QMAS spectrum compared with the MAS spectrum, because this species has a very weak quadrupoplar interaction and is therefore, not well excited in the MQMAS transfers [21].

To summarize, for the calcined Mo–Al samples, the ^{27}Al 3QMAS NMR results are similar whatever the method of preparation.

3.1.3. MoP–Al samples: dried state

Two amounts of phosphorus (atomic ratio P/Al = 0.03 and 0.2) were studied for a fixed amount of molybdenum (atomic ratio Mo/Al = 0.2).

Concerning the dried solids, the XRD patterns show broad peaks similar for Mo1P1–Al, Mo1P3–Al, Mo3P1–Al and Mo3P3–Al whatever the atomic ratio (P/Al = 0.03 or 0.2). These patterns are characteristic for the presence of poorly crystallised boehmite.

Table 3 reports the samples composition of the dried MoP–Al solids, in which the carbon amount varies from 6.1 to 9.2 wt.%.

The ^{27}Al spectra of the dried MoP(0.03)–Al samples are reported in Fig. 5A. Whatever the method of preparation, the NMR spectra are characteristic for octahedral aluminium. The ^{31}P NMR spectra leads to broad signals. By comparison of the shift of the peak, the presence of monomeric or polymeric phos-

Table 2
Averaged δ_2^G (resonance frequency), δ_{CS} (chemical shift) and SOQE values obtained by ^{27}Al 3QMAS NMR of the Mo(0.2)C–Al and Mo(0.3)C–Al sample series

	δ_2^G (ppm)	δ_{CS} (ppm)	SOQE (MHz)	δ_2^G (ppm)	δ_{CS} (ppm)	SOQE (MHz)
	Mo1(0.2)C–Al			*Mo3(0.2)C–Al*		
S1	5.5	12	3.5	6	12	3.3
S2	29	39	4.3	29	39	4.3
S3	64	75	4.5	65	74	4.4
	Mo1(0.3)C–Al			*Mo3(0.3)C–Al*		
S1	5.1	12	3.4	5.8	12	3.3
S2	29	39	4.4	29	39	4.3
S3	64	75	4.5	64	74	4.2
S4				−13	−12.9	0.5

Table 3
Chemical composition of Mo–P–Alumina samples in the dried and calcined states and SSA

Catalysts	wt.% C		wt.% Mo		Mo/Al	wt.% P		SSA (m^2/g)
	D	C	D	C	D and C	D	C	C
Mo1(0.2)P1(0.03)	7.3	0.1	13.4	21.4	0.2	1.4	1.5	378
Mo1(0.2)P3(0.03)	6.8	0.1	14.4	21.3	0.2	1.2	1.6	–
Mo3(0.2)P1(0.03)	9.2	0.2	13.2	19.4	0.2	1.1	1.2	–
Mo3(0.2)P3(0.03)	9.0	0.3	13.0	18.4	0.2	1.0	1.1	–
Mo1(0.2)P1(0.2)	6.8	0.2	11.7	18.0	0.2	6.1	7.3	314
Mo1(0.2)P3(0.2)	6.1	0.4	11.8	17.7	0.2	5.4	7.8	–
Mo3(0.2)P1(0.2)	6.9	0.2	12.1	16.0	0.2	5.7	7.0	391
Mo3(0.2)P3(0.2)	7.0	0.3	10.9	15.8	0.2	5.2	6.9	389

D = dried state, C = calcined state; SSA determined after calcination at 500°C.

Table 4
^{31}P NMR chemical shift of the Mo–P samples in the dried and the calcined state

	Mo1P1–Al	Mo3P1–Al	Mo1P3–Al	Mo3P3–Al
P / Al = 0.03				
Dried	−16.3	−13	−16.8	−12.5
Calcined	−21.1	−17.7	−24.1	−21.9
P / Al = 0.2				
Dried	−25	−22.2	–	−16.6
Calcined	−26.5	−25.8	–	−17

phates species, as well as aluminium phosphate, can be determined. For the MoP(0.03)–Al series, two groups can be distinguished (Table 4): samples Mo3P3–Al and Mo3P1–Al for which the top of the peak is around −13 ppm, indicating, essentially, the presence of monomeric phosphates, and Mo1P1–Al and Mo1P3–Al with the maximum around −16 ppm corresponding to polymeric phosphates.

For the MoP(0.2)–Al series (Fig. 5B), ^{27}Al NMR MAS spectra show the presence of the octahedral aluminium sites and the formation of a new species around 39 ppm corresponding to Al species in $AlPO_4$. Moreover, there are some differences in the intensity and the shape of the peak corresponding to $AlPO_4$. Concerning the ^{31}P NMR, we can observe an evolution toward the polymeric phosphates compared to the MoP(0.03)–Al samples (Table 4) as the peak maximum shifts to lower values with the exception of sample Mo3P3, which has more dispersed phosphates species (−16.6 ppm).

3.1.4. MoP–Al samples: calcined state

Concerning the calcined solids, the XRD patterns of the Mo3P3, Mo1P3 and Mo3P1 samples are

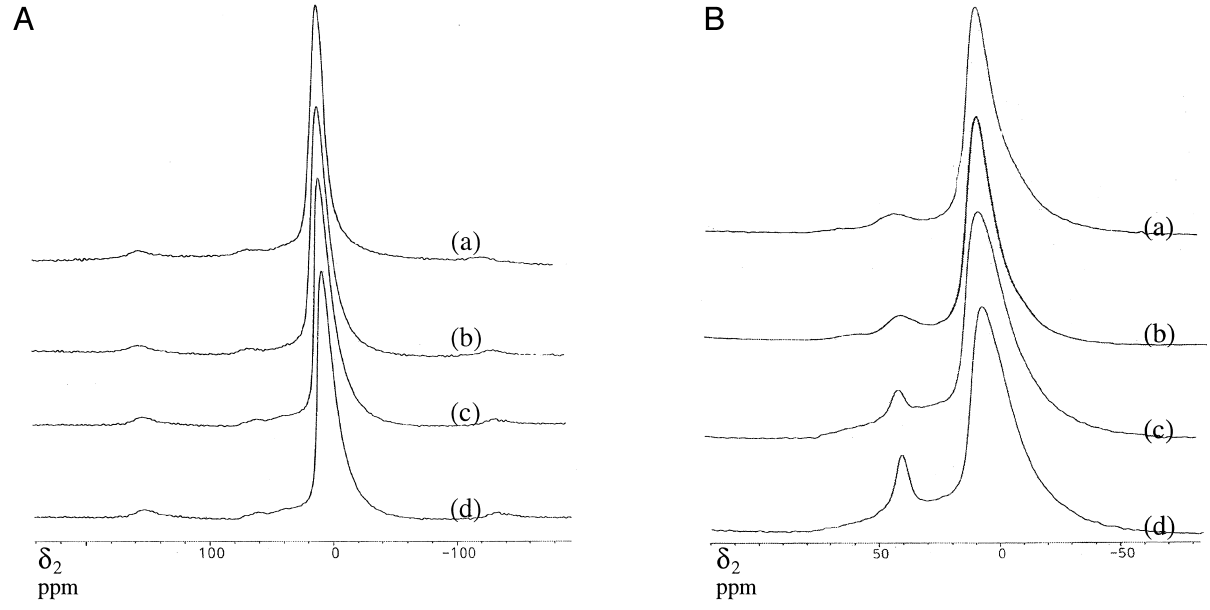

Fig. 5. ^{27}Al MAS NMR spectra of the dried MoP–Al solids. (A) (a) Mo3P3(0.03)–Al, (b) Mo3P1(0.03)–Al, (c) Mo1P3(0.03)–Al, (d) Mo1P1(0.03)–Al. (B) (a) Mo3P3(0.2)–Al, (b) Mo3P1(0.2)–Al, (c) Mo1P3(0.2)–Al, (d) Mo1P1(0.2)–Al.

similar (badly crystallised γ-alumina). On the contrary, for Mo1P1, the presence of the characteristic signal of $AlPO_4$, as it was already detected in the P3–Al sample [5], can be noted. As for the Mo–Al calcined samples, the amount of carbon is very low after calcination (less than 0.4 wt.%; Table 3) and SSA remains always higher than 300 $m^2\ g^{-1}$.

The ^{27}Al MAS NMR of the calcined Mo1P1-(0.03)–Al, Mo3P1(0.03)–Al, Mo1P3(0.03)–Al and Mo3P3(0.03)–Al are reported in Fig. 6A. The spectra of samples Mo1P3–Al and Mo3P1–Al are quite similar to those of Mo1P1–Al and Mo3P3–Al, which were already described [16]. The three characteristic species (octahedral, tetrahedral and pentacoordinate aluminium) are clearly evidenced. The ^{31}P MAS NMR spectra show essentially polymeric phosphates whatever the method of preparation (Table 4).

Concerning the higher amount of phosphorus (P/Al = 0.2), the ^{27}Al NMR spectra show the formation of a species around 39 ppm in each case (Fig. 6B). Nevertheless, the intensity and the shape of the signal are different, as already noted for the corresponding dried solids. ^{31}P MAS NMR does not show large differences between Mo1P1, Mo3P1, with the presence of polymeric phosphate and aluminium phosphates (−26 ppm), whereas for Mo3P3 (−17 ppm), phosphorus seems to be better dispersed with less aluminium phosphates.

For this series of MoP–Al samples, 3QMAS experiments were performed as for the Mo–Al catalysts. In a previous work [16], it was shown that the structures of Mo1P1–Al and Mo3P3–Al are different. Indeed, for Mo1P1–Al, up to five different aluminium species were detected; they correspond to octahedral, pentacoordinate, tetrahedral aluminium and two $AlPO_4$ species, one of which is a well-crystallised $AlPO_4$ phase. For sample Mo3P3–Al, we observed four different species in which phophorus is in a local environment different than in Mo1P1–Al. Here, the study is completed with Mo1P3–Al and Mo3P1–Al catalysts, and reproducibility in the measurements was checked. Indeed, no large deviation was found between the published results [16] and the value reported in the present paper. Fig. 7 reports the high resolution 1D spectrum (projection of the 2D 3QMAS spectrum on the δ_{iso} axis) of the Mo1P1–Al, Mo3P3–Al, Mo1P3–Al and Mo3P1–Al samples. Mo1P3–Al is similar to Mo3P3–Al and Mo1P1–Al is similar to Mo3P1–Al. Clearly, an additional species is detected when the phosphorus is dissolved

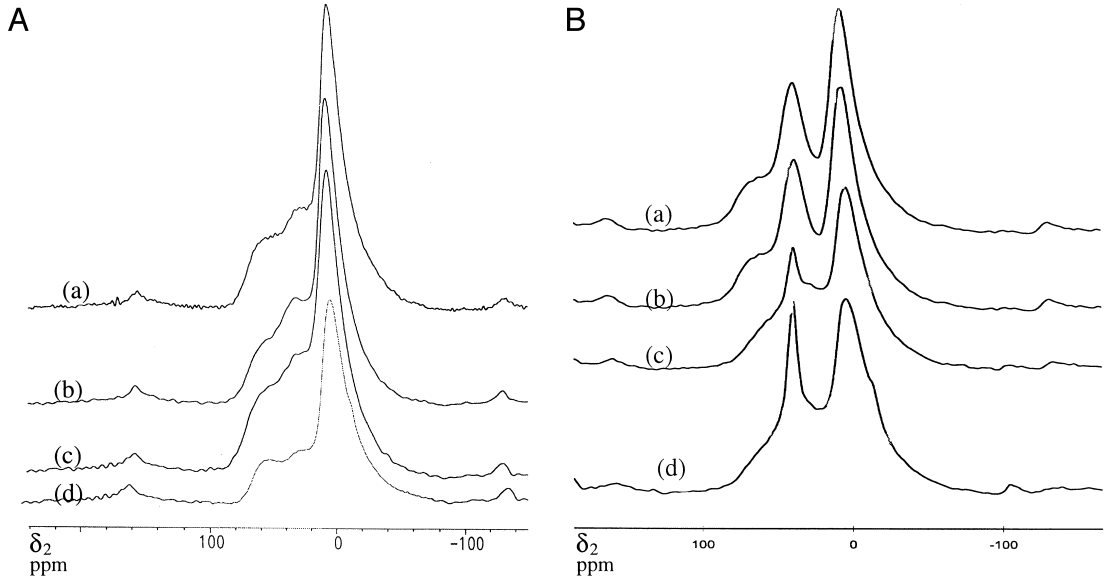

Fig. 6. ^{27}Al MAS NMR spectra of the calcined MoP–Al solids. (A) (a) Mo3P3(0.03)–Al, (b) Mo3P1(0.03)–Al, (c) Mo1P3(0.03)–Al, (d) Mo1P1(0.03)–Al. (B) (a) Mo3P3(0.2)–Al, (b) Mo3P1(0.2)–Al, (c) Mo1P3(0.2)–Al, (d) Mo1P1(0.2)–Al.

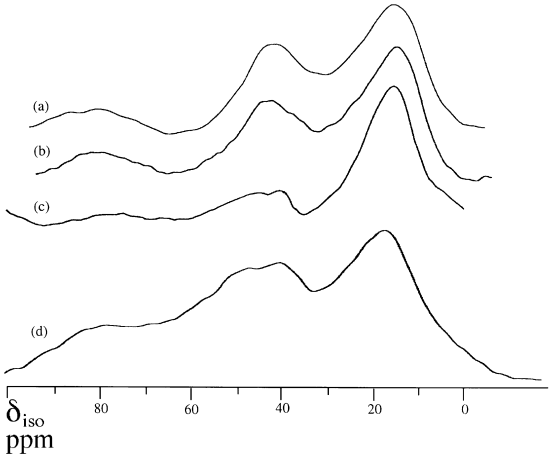

Fig. 7. High resolution 1D spectrum. (a) Mo3P3(0.2)–Al, (b) Mo1P3(0.2)–Al, (c) Mo3P1(0.2)–Al, (d) Mo1P1(0.2)–Al.

in step 1 (2-butanol). The corresponding isotropic chemical shifts and the SOQE are reported in Table 5. There is no doubt that the number of aluminium species changes with the method of preparation with, in addition, some differences observed in the local environment of each site. From Table 5, it is possible to compare the results obtained for Mo1P1–Al and Mo3P1–Al in one hand, and Mo1P3–Al and Mo3P3–Al in the other. There is no difference in the SOQE values of the octahedral site (S1) whatever the method of preparation (SOQE ≈ 3.4 MHz). For S2 assigned to a probably pentacoordinate species, the SOQE value cannot be evaluated. The species S3 corresponds to the tetrahedral aluminium site. Its SOQE values are in the same order (SOQE ≈ 5.0 MHz) whatever the method of preparation, but are quite higher than the values obtained for the Mo–Al catalysts.

For Mo3P1–Al and Mo1P1–Al, a species S4 ($\delta_2^G = 40$ ppm) is also observed with the same weak quadrupolar interaction (SOQE ≈ 1.5 MHz). This means that the species (probably aluminium in $AlPO_4$) are in the same electronic environment in both samples. Signal S5 for Mo3P1–Al and Mo1P1–Al seems to be the same species for both samples ($\delta_2^G = 45$ ppm and SOQE ≈ 3.5 MHz).

On the contrary, for Mo1P3–Al and Mo3P3–Al, when the phosphorus is dissolved in water, the species S4 ($\delta_2^G = 36$ ppm and SOQE ≈ 2.4 MHz) seems to be different from the S4 species observed in the Mo3P1–Al and Mo1P1–Al samples. The electronic environment of this aluminium site indicates a better local structure organisation in samples Mo1P3–Al and Mo3P3–Al.

In short, phosphorus seems to play an essential role on the structure of the alumina framework. The introduction of phosphorus in water or in butanol leads to aluminium sites with different environments, and probably, to different species.

3.2. Thiophene HDS activity

3.2.1. Mo–Al catalysts

Fig. 8 shows the HDS activity of the Mo1C–Al and Mo3C–Al catalysts with different amounts of

Table 5
Averaged δ_2^G (resonance frequency), δ_{CS} (chemical shift) and SOQE values obtained by ^{27}Al 3QMAS NMR of the Mo(0.2)P(0.2)C–Al sample series

	δ_2^G (ppm)	δ_{CS} (ppm)	SOQE (MHz)	δ_2^G (ppm)	δ_{CS} (ppm)	SOQE (MHz)
	Mo3(0.2)P1(0.2)–Al			*Mo1(0.2)P3(0.2)–Al*		
S1	5.6	12	3.4	5.8	12	3.4
S2	29	39	[a]			
S3	59	73	5.1	58	72	5.1
S4	40	41	1.5	36	39	2.4
S5	38	45	3.5			
	Mo1(0.2)P1(0.2)Al			*Mo3(0.2)P3(0.2)–Al*		
S1	5.4	12	3.5	6.1	12	3.3
S2	29	39	[a]			
S3	59	73	5.0	59	73	5.0
S4	40	41	1.6	36	39	2.4
S5	38	45	3.6			

[a] Undetermined: low intensity, overlapping resonances.

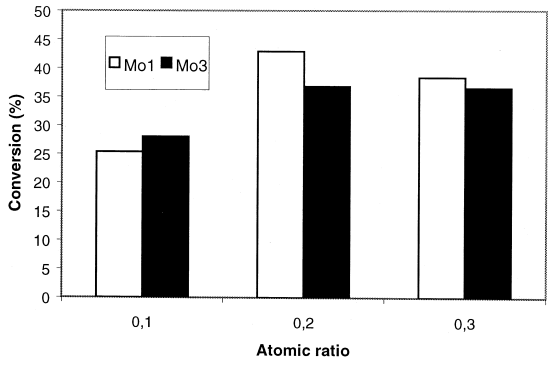

Fig. 8. Thiophene HDS activity of Mo1C–Al and Mo3C–Al catalysts for different Mo/Al atomic ratio.

molybdenum (atomic ratio Mo/Al = 0.1, 0.2, 0.3). The HDS conversion increases with the amount of molybdenum. For the Mo1C–Al samples, a maximum around 20 wt.% Mo (atomic ratio Mo/Al = 0.2) appears, whereas for the Mo3C–Al series, HDS activity is constant for Mo/Al = 0.2 and 0.3.

Clearly, the method of preparation of the Mo–Al catalysts induces variation in the HDS performances. For samples with high Mo content (Mo/Al = 0.2 and 0.3), the catalytic activity for thiophene HDS follows the trend: Mo1–Al > Mo3–Al. On the contrary, for low Mo content (Mo/Al = 0.1), the reverse trend is observed: Mo3–Al > Mo1–Al. Such variations can be correlated with the detection by NMR of Al species in a $Al_2(MoO_4)_3$ structure for samples prepared with Mo introduced with water (step 3) in high amount (sample Mo3(0.3)C–Al, see Fig. 3f).

3.2.2. MoP–Al catalysts

Fig. 9 shows the HDS thiophene conversion of the mixed Mo–P–Al samples. The four tested catalysts have the same Mo/Al ratio (Mo/Al = 0.2) and the same P/Al ratio (P/Al = 0.2). Therefore, as the activity in HDS is always correlated to the presence of Mo (formation of the MoS_2 active phase after activation) [2], the performances of these catalysts have to be compared with samples Mo1(0.2)–Al and Mo3(0.2)–Al of Fig. 8. The trend in Fig. 9 is the following: Mo3P3–Al > Mo1P3–Al > Mo1P1–Al > Mo3P1–Al, with, however, two classes. The first class of catalysts (Mo3P3–Al and Mo1P3–Al) has a higher activity than the corresponding Mo1(0.2)–Al and Mo3(0.2)–Al (Fig. 8): they are both prepared by the introduction of phosphorus in step 3 of the procedure (Fig. 1). On the contrary, the second class of catalysts (Mo1P1–Al and Mo3P1–Al) has a slightly lower activity than the corresponding phosphorus free catalysts: they are both prepared by the introduction of phosphorus in step 1 of the procedure (Fig. 1).

Clearly, the way of introduction of the phosphorus precursor in the gel genesis makes it a promotor (step 3) or an inhibitor (step 1) of the Mo active phase.

3.3. Characterization of the sulfided state

In order to have a clear view between the NMR characterization of the Mo–Al and MoP–Al samples in the calcined state and the catalytic performances of the corresponding sulfided catalysts, some NMR characterizations have been undertaken (Fig. 10) on some sulfided catalysts, which have been catalytically tested. It is obvious that air exposure of the catalysts before the NMR experiments and after the HDS test may provoke some reoxidation of the active phase. Nevertheless, a comparison of the ^{27}Al MAS NMR spectra of samples in Fig. 10 with the corresponding ones in Figs. 3 and 6 deserves some interest.

Clearly, it is observed that there are no great difference between the calcined and the sulfided states for the Mo–Al and MoP–Al catalysts. This study cannot give an information on the active phase, but the important fact is that the structure of the alumina is not apparently destroyed by the sulfidation and testing procedure.

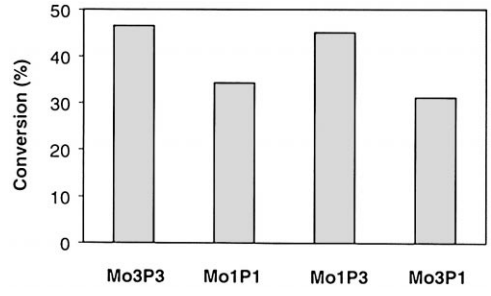

Fig. 9. Thiophene HDS activity of MoP(0.2)C–Al catalysts.

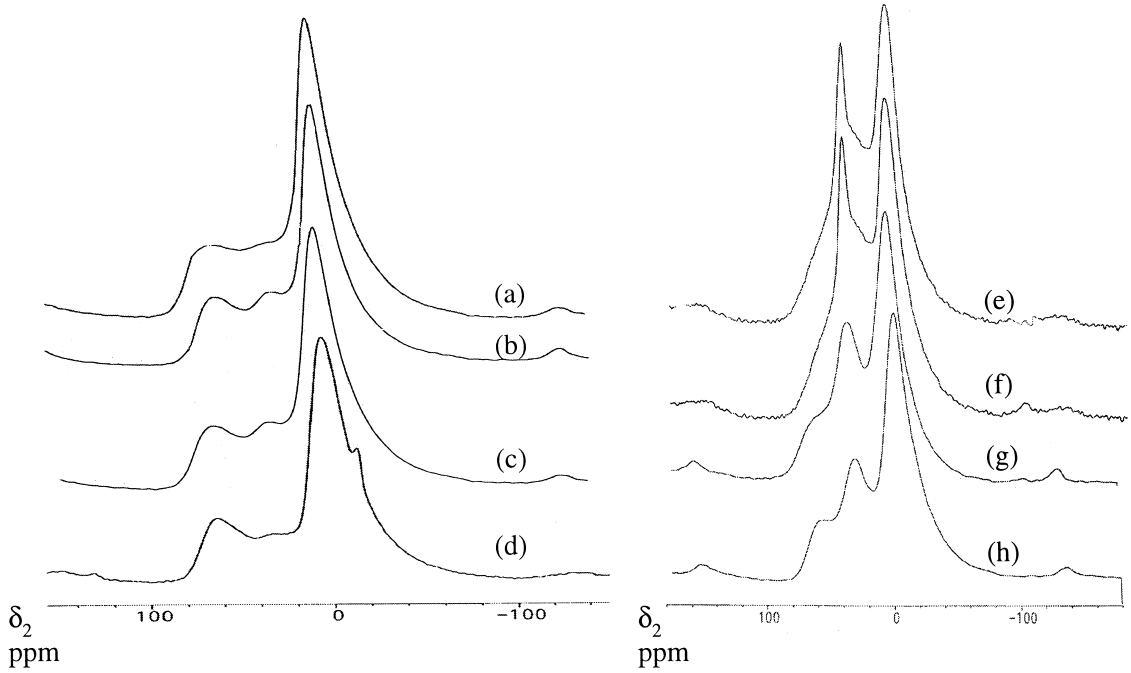

Fig. 10. ^{27}Al MAS NMR spectra after the catalytic test. (a) Mo1(0.2)–Al, (b) Mo3(0.2)–Al, (c) Mo1(0.3)–Al, (d) Mo3(0.3)–Al, (e) Mo1P1(0.2)–Al, (f) Mo3P1(0.2)–Al, (g) Mo1P3(0.2)–Al, (h) Mo3P3(0.2)–Al.

Moreover, it seems that after sulfidation, the $Al_2(MoO_4)_3$ content decreases in the Mo3(0.3)–Al catalysts (compare spectrum d of Fig. 10 with spectrum f of Fig. 3).

4. Discussion

One of the most important observations of the present work is the influence of the method of catalysts preparation. The characteristics of the oxide phase (after calcination) are different when the element molybdenum or phosphorus is introduced in step 1 (2-butanol) or in step 3 (water). In fact, the important step seems to be the introduction of phosphorus. Its introduction in step 1 (see Fig. 1) leads to the formation of a well-crystallised $AlPO_4$ phase, when the molybdenum is introduced either in 2-butanol (step 1) or in water (step 3). When phosphorus is introduced with water, the presence of the species around $\delta_2^G = 39$ ppm, observed in 3QMAS, seems to be due to the formation of a new phase; we have already proposed [16] the formation of "Mo–O–P" compounds and other characterizations [26] seem to confirm this result.

Another interesting result concerns the influence of the association between phosphorus and molybdenum. In a previous study on P–Al solids [5], it was shown that when phosphorus was introduced in water (P3(0.2)–Al), there was formation of a well-crystallized $AlPO_4$ phase. This phase was not present in the case of P1–Al (introduction of phosphorus in 2-butanol). The present study shows that in the case of the association of Mo with P, the formation of $AlPO_4$ occurs mainly when the phosphorus precursor is dissolved in 2-butanol, whatever the step of introduction of molybdenum. So, the association of molybdenum and phosphorus induces the formation of $AlPO_4$. On the contrary, when the phosphorus precursor is introduced in water in association of molybdenum, there is no formation of $AlPO_4$. The main conclusion is that phosphorus has a much more important influence than molybdenum on the structure of the MoP–Al catalysts prepared by a sol–gel method.

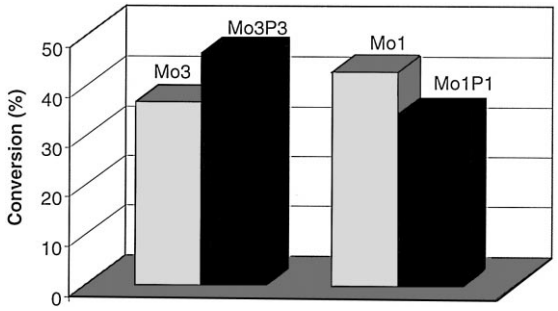

Fig. 11. Evidence of poisoning or promoting effects of phosphorus in MoP–Al catalysts.

Concerning the catalytic performances of the prepared (and activated) solids, there is a good correlation between the characterization of the oxide and the HDS of thiophene. Indeed, the maximum of conversion of the MoP–Al catalysts is obtained when the phosphorus precursor is dissolved in water (Mo3P3–Al and Mo1P3–Al). This can be correlated with the formation of the catalytic phase, the precursors of which are associated to "Mo–O–P" species. The fact that the Mo1P1–Al and Mo3P1–Al are less active can also be due to the formation of the $AlPO_4$ phase, and also, to the presence of $Al_2(MoO_4)_3$ for some sol–gel preparations. This result underlines the importance of the control of the oxide preparation for the catalytic performances exhibited by the corresponding sulfided solids.

The promotor effect of phosphorus on the Mo-based active phase can be also discussed in the light of the results shown in Fig. 11.

Phosphorus has a poisoning effect in the case of Mo1P1–Al by reference to Mo1–Al and a promoting effect by reference to Mo3–Al. In the first case, we can attribute the decrease of the activity by either the formation of $AlPO_4$ or $Al_2(MoO_4)_3$. In the comparison of Mo3–Al with Mo3P3–Al, the promoting effect is clear. Moreover, the effect of phosphorus is also positive when comparing Mo3P3–Al and Mo1–Al. Therefore, the step of introduction of phosphorus in the sol–gel method is very important for the preparation of the MoP–Al catalysts.

5. Conclusion

In this work, Mo–Al and MoP–Al catalysts prepared by a sol–gel method have been extensively characterized by solid state NMR. We were particularly interested in the modifications induced on the dried and calcined samples by the step of introduction of molybdenum and phosphorus. We have shown that the structure of the alumina framework greatly depends on the step of introduction of the phosphorus with the formation of a new $AlPO_4$ phase when phosphorus is dissolved in water. The initial structure of the oxide has an important influence on the catalytic behaviour of the solids after activation by sulfidation. Particularly, for the MoP–Al catalysts, we have observed a promotor effect when phosphorus is dissolved in water, whatever the step of introduction of molybdenum (in 2-butanol or in water).

Acknowledgements

The authors thank B. Revel from the Centre Commun de Mesures RMN de l'Université des Sciences et Technologies de Lille for its help and technical support and Dr. R. Bechara for the determination of the SSA of the catalysts. The Région Nord Pas de Calais is also acknowledged for a financial support for the purchase of the ASX400 and ASX100 spectrometers. Bruker is also acknowledged for his scientific collaboration.

References

[1] J. Grimblot, Catal. Today 41 (1998) 111.
[2] H. Topsøe, B.S. Clausen, F.E. Massoth, Hydrotreating Catalysis, Springer-Verlag, Berlin, 1996, and references therein.
[3] E. Etienne, E. Ponthieu, E. Payen, J. Grimblot, J. Non-Cryst. Solids 147–148 (1992) 764.
[4] L. Le Bihan, C. Mauchaussé, L. Duhamel, J. Grimblot, E. Payen, J. Sol–Gel Sci. Technol. 2 (1994) 837.
[5] J. Quartararo, C. Fernandez, M. Guelton, M. Rigole, J.P. Amoureux, J. Grimblot, J. Mater. Chem. 9 (1999) 2637.
[6] R. Iwamoto, J. Grimblot, Adv. Catal. 44 (1999) 417.
[7] R. Iwamoto, J. Grimblot, Stud. Surf. Sci. Catal. 106 (1997) 195.
[8] R. Iwamoto, J. Grimblot, J. Catal. 172 (1997) 252.
[9] J.L.G. Fierro, A. López Agudo, N. Esquivel, R. López Cordero, Appl. Catal. 48 (1989) 353.
[10] R. López Cordero, N. Esquivel, J. Lazzaro, J.L.G. Fierro, A. López Agudo, Appl. Catal. 48 (1989) 341.
[11] P.J. Mangnus, J.A.R. van Veen, S. Eijbouts, V.H.J. de Beer, J.A. Moulijn, Appl. Catal. 61 (1990) 99.

[12] J.M. Lewis, R.A. Kydd, R.M. Boorman, P.H. van Rhyn, Appl. Catal. A 84 (1992) 103.
[13] A. Lopez Agudo, Appl. Catal. A 161 (1997) 105.
[14] M. Jian, R. Prins, Catal. Lett. 35 (1995) 193.
[15] R. Iwamoto, C. Fernandez, J.P. Amoureux, J. Grimblot, J. Phys. Chem. B 102 (1998) 4342.
[16] J. Quartararo, M. Rigole, M. Guelton, J.P. Amoureux, J. Grimblot, J. Chim. Phys. 96 (1999) 1536.
[17] J.P. Amoureux, C. Fernandez, S. Steuernagel, J. Magn. Reson., Ser. A 123 (1996) 116.
[18] C. Fernandez, J.P. Amoureux, J.M. Chezeau, L. Delmotte, H. Kessler, Microporous Mater. 6 (1996) 331.
[19] A. Medek, J.S. Hardwood, L. Frydman, J. Am. Chem. Soc. 117 (1995) 12779.
[20] D. Massiot, B. Touzo, D. Trumeau, J.P. Coutures, J. Virlet, P. Florian, P.J. Grandinetti, Solid State Nucl. Magn. Reson. 6 (1996) 73.
[21] J.P. Amoureux, C. Fernandez, Solid State Nucl. Magn. Reson. 10 (1998) 211.
[22] Y. Kurokawa, Y. Kobayashi, S. Nakaka, Heterog. Chem. Rev. 1 (1994) 309.
[23] S.H. Risbud, R.J. Kirkpatrick, A.P. Tagliavore, B. Montez, J. Am. Ceram. Soc. 70 (1987) C10.
[24] J. Leyer, M.I. Zaki, H. Knözinger, J. Am. Chem. Soc. 90 (1986) 4775.
[25] R. Thomas, F.P.J.M. Kerkohof, J.A. Moulijn, J. Medema, V.H.J. de Beer, J. Catal. 61 (1980) 559.
[26] J. Quartararo, L. Duhamel, J. Grimblot, unpublished results.